Theor Appl Climatol
DOI 10.1007/s00704-015-1382-5

ORIGINAL PAPER

# Determining changes in the average minimum winter temperature of Horqin Sandy Land using tree ring records

**Long Ma · TingXi Liu · JingRu Wang · LanHong Ji · RuiZhong Gao**

Received: 22 July 2014 / Accepted: 19 January 2015


**Abstract** Horqin Sandy Land, a region in China that suffers from desertification, has become a primary economic zone in Inner Mongolia MengDong. Ecological and environmental problems continue to affect the local environment and human survival, becoming one of the bottlenecks to economic and social development. Thus, research on the characteristics of climatic variation is urgently required. This study used the comprehensive timeline for the regional tree wheel width of Horqin Sandy Land to reconstruct the average minimum winter temperatures of the study area. The timeline, which has been in use for 183 years, was established using core samples from the annual growth rings of elm trees in 10 sampling sites. For 181 years (1826–2006), varying minimum temperatures were observed: a gentle wave stage (1826–1923), an intense cooling stage (1923–1957), and a considerable heating stage (1957–2006). The longest continuous heating stage was observed from 1957 to 2006, during which time the average minimum temperature was −16.81 °C, a value greater than the mean temperature over the entire study period. The coldest 10 years occurred during the 1950s, until 1957, at which point the temperature sharply increased. The next 50 years exhibited a general warming trend until 2000. This period reflected a time span with the warmest minimum temperature and displayed a warming trend rate of 0.575 °C/10 years and an overall increase of up to 1.5° every 50 years. A continued rise in temperature is predicted to cause a wider range and longer time scale of ecological and environmental problems.

L. Ma (✉) · T. Liu · J. Wang · L. Ji · R. Gao
Water Conservancy and Civil Engineering College, Inner Mongolia Agricultural University, Hohhot, Inner Mongolia 010018, China
e-mail: malong4444333@163.com

T. Liu
e-mail: Liutingxi66@163.com

J. Wang
e-mail: 339199034@qq.com

L. Ji
e-mail: jihonglan123@126.com

R. Gao
e-mail: grzh2009@sohu.com

## 1 Introduction

China is one of the many countries experiencing severe desertification. The rapid progression of dryland degradation has become an important ecological and socioeconomic problem (Wang et al. 2002; Wang and Zhu 2001). Horqin Sandy Land (Fig. 1) is one of the four major sandy land areas in China that exhibit typical changes in climate and surface environment. Studies on the desertification process and its mechanism have aided the understanding of the environmental degradation in Horqin Sandy Land (Wang and Zhu 2001; Dong et al. 1998; Wang et al. 2004b, c; 2006; Li et al. 2007; Zhao et al. 2008). Wang et al. (2004c) reported that the different precipitation and temperature combinations observed from the 1960s to 2000 have influenced the desertification process. Desertification is the result of 1100 years of climate fluctuations (Dong et al. 1998).

Climate change has imposed severe effects on the ecological environment of Horqin Sandy Land, signaling the necessity for research on climate change in relation to this region. Numerous climate change studies on Horqin Sandy Land and its surrounding areas have been conducted (Zhai and Pan 2003; Wang et al. 2004a). However, these studies have focused on the time period from the 1950s to the beginning of the 21st century, with discussions detailing the variations in precipitation (Chen et al. 2004; Zhang and Zhang 2005; Yi et al. 2006; Liang et al. 2009), average temperature (Sun

Published online: 04 February 2015

et al. 2006; Hou et al. 2006; Wang et al. 2007a, b), and average highest/lowest temperature (Wang et al. 2004a; Sun et al. 2006; Wang et al. 2007a, b), among others. In these investigations, a fixed number of years and smaller regional study sites were considered; as a result, the discussion of climate change over these small time scales is no longer sufficient for understanding current situations. Tree ring records reveal accurate climate information, making the analysis of such data an effective means of understanding climate change problems.

Tree ring-based reconstructions present information that feature accurate positioning, good continuity, high resolution, and precise correlation with climate change (Fritts 1976; Shao 1997; Nicoletta 2004). Many scholars have used tree ring data to reconstruct long-term climate information, covering aspects such as temperature and rainfall (Esper et al. 2003; Law et al. 2006; Giovanna et al. 2010). These data have also been applied to research on hydrological events, including ice-jam flooding, volcanic eruptions, and surface runoff (Stockton and Meko 1975; Cook and Jacoby 1983; Van Arsdale et al. 1998; Magda et al. 2001). In China, a study on timeline establishment and climate reconstruction was carried out in Tibet, Inner Mongolia and other regions, focusing on Sabina przewalskii and Ulmus pumila L. as the research objects (Zhuo et al. 1979; Ma et al. 2011). Wu et al. (1989) used tree ring data to reconstruct past climate changes in central Tibet. Shao et al. (2007) established a 3500-year master tree ring chronology for the northeastern part of the Qaidam Basin. In addition, previous studies (Ma et al. 2007; Ma et al. 2011) have established ring width chronology and elm reconstruction for Horqin Sandy Land. Nevertheless, these studies focused primarily on reconstructing climate change in the region-near sampling sites, using tree ring networks as the bases of research. This approach is relatively rare.

The existence of global warming is indisputable (Wang 1994; Wang et al. 2005). In recent years, the annual average temperature in China has increased between 0.5 and 0.8 °C (Ding et al. 2006), and the changes in the maximum and minimum temperatures of some areas reflect an asymmetric trend (Karl et al. 1993; Xie and Cao 1996; Ma 1999). Warming occurs mainly during the evening in most parts of the northern hemisphere (Karl et al. 1993). Global warming mostly represents an increase in the lowest temperature or rising temperatures at night. Wilson and Luckman (2003) emphasized that broader temperature variables, such as maximum and minimum temperatures, should be reconstructed. Malone (cited in Ma et al. 2011) established a 183-year ring width chronology and reconstruction of elm in Horqin Sandy Land. In the current work, we use this chronology to reconstruct the average minimum winter temperature in the region and discuss the variation characteristics of minimum temperature.

## 2 Study area and data

### 2.1 Study area

The average annual precipitation in Sandy Land is 200–650 mm, with rainfall from June to August accounting for 70 % of annual precipitation. The multi-year average evaporation is 1600–2400 mm (evaporation pan diameter, 20 cm), with evaporation from April to September accounting for 78 % of annual evaporation. In this area, summers are hot and winters are dry, cold, and long. The multi-year average temperature is 6 °C. Fixed sandy lands, semi-fixed sandy lands, and migratory dunes characterize the landform in this region. The largest area is covered with aeolian sand, and smaller regions are covered with meadow and chestnut soil. Halomorphic, dark brown, chernozem, chestnut-cinnamon, skeleton, cinnamon, bog, and alluvial soils are also present. Plant species are abundant, representing a broad range of flora from Mongolia (North China) to Changbai, where the most widely distributed plants can be found (Jiang et al. 2003).

### 2.2 Chronological data

A ring width chronology and reconstruction of elm in Sandy Land were used (Ma et al. 2011). The distribution of meteorological stations in the study site and its surrounding areas are shown in Fig. 1. The 10 meteorological stations are listed in Table 1, and the established ring width chronology for 1826–2008 (183 years) is shown in Fig. 2 (Ma et al. 2011).

### 2.3 Meteorological data

The 1951–2008 average temperature, precipitation, and maximum/minimum temperatures of the 10 elm sampling sites were obtained from the eight meteorological stations closest to the sites: Horqin Left Back Banner, TongLiao, Kailu, Horqin Left Middle Banner, Jarud Qi, Horqin Right Middle Banner, Horqin Left Right Banner, and Kulun. Data from adjacent sites were used to interpolate measurements where data from the above stations were incomplete. The uniformity of each meteorological element indicates that the temperature, precipitation, and meteorological data from the sites did not exhibit significant deviations or random changes, and that data changes were relatively homogenous and consistent. Thus, the data were considered a reliable representation of the climate conditions in the region.

## 3 Reconstruction of average minimum winter temperature

### 3.1 Response relationship of the chronological and climatic factors

The monthly maximum temperature, minimum temperature, mean temperature, and monthly (annual) precipitation

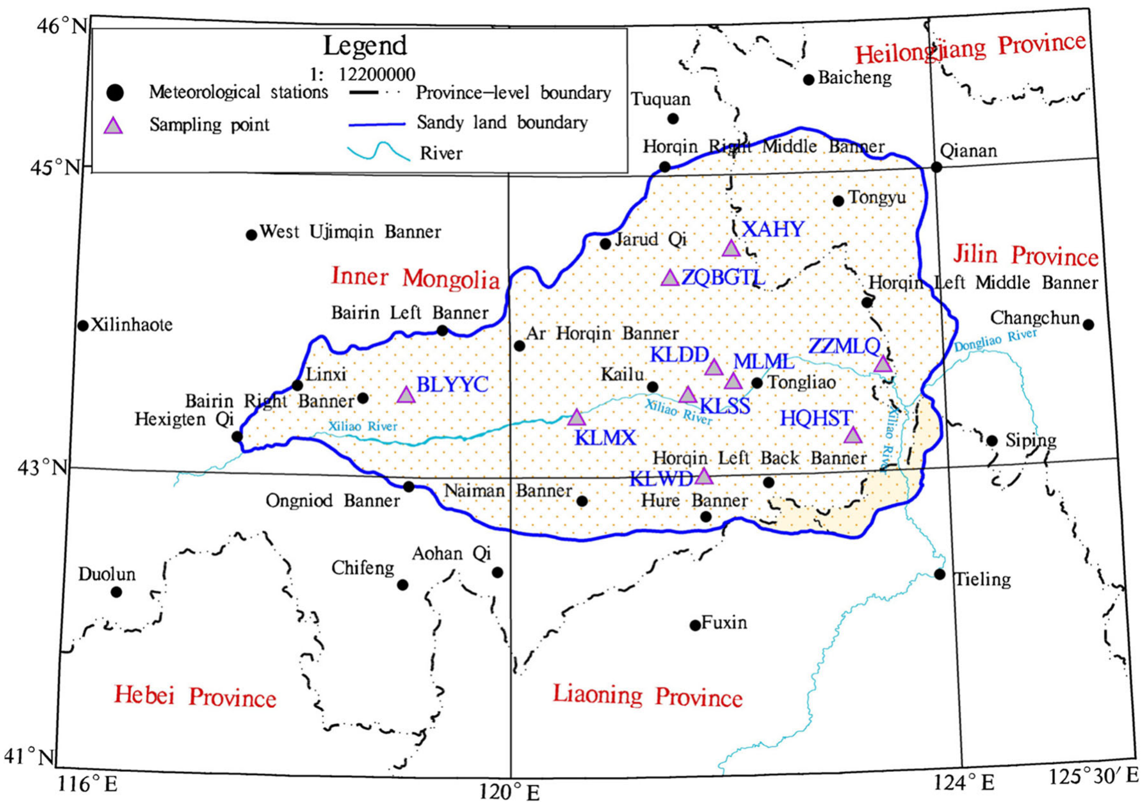


**Fig. 1** Range of Horqin Sandy Land, tree ring sample sites, and the distribution of meteorological stations in surrounding areas

registered by the eight sites were divided equally to represent the average regional climate in Horqin Sandy Land.

Tree ring climatology considers that (Fritts 1976) the rings formed in year $t$ are influenced not only by the climate at that time but also by the climate during the previous 1–2 years. Therefore, the standard chronological sequence and standard chronological $t+1$ and $t+2$ sequences in relation to the monthly maximum temperature, minimum temperature, monthly mean temperature, and monthly (annual) precipitation series in Horqin were analyzed. The correlation coefficient is shown in Fig. 3.

As shown in Fig. 3, the study area is a typical arid and semi-arid region, exhibiting less precipitation during the early tree-growing season (April and May). Water is crucial to tree growth before the leaves turn green, and more precipitation in February and March provides a solid foundation for the layer

**Table 1** Descriptive information for sampling sites

| ID | Code | North latitude/° | East longitude/° | Altitude/m | Sample size/plant/core | Sample length/a |
|---|---|---|---|---|---|---|
| 1 | KLDD | 43.66 | 121.83 | 207 | 26/52 | 119 |
| 2 | MLML | 43.59 | 122.02 | 193 | 23/43 | 122 |
| 3 | KLSS | 43.54 | 121.55 | 224 | 12/24 | 203 |
| 4 | HQHST | 43.19 | 123.04 | 159 | 25/47 | 145 |
| 5 | ZZMLQ | 43.67 | 123.42 | 134 | 22/44 | 125 |
| 6 | KLWD | 42.98 | 121.69 | 291 | 21/42 | 206 |
| 7 | XAHY | 44.50 | 122.00 | 180 | 23/46 | 136 |
| 8 | ZQBGTL | 44.33 | 121.58 | 204 | 24/43 | 155 |
| 9 | KLMX | 43.41 | 120.59 | 343 | 26/52 | 138 |
| 10 | BLYYC | 43.53 | 118.83 | 506 | 28/56 | 132 |
| Total | | | | | 230/449 | |

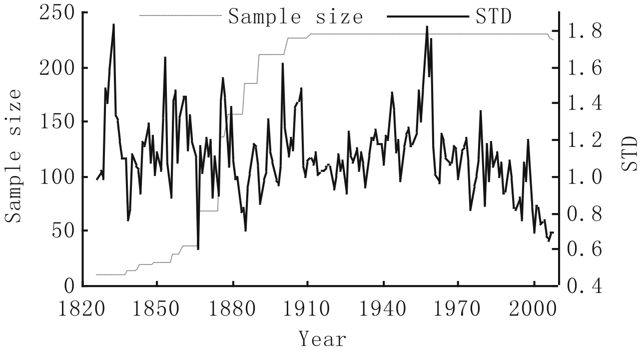


**Fig. 2** Regional elm STD chronologies and sample sizes

of elm wood cells. The cells then begin to produce secondary wood cells. The dependence of elm on water further increases during the initial growth stage (April and May). In this period, abundant precipitation can replenish the water required for the trees to promote the differentiation of secondary elm wood cambium cells and form part of the spring material (or early wood). Summer (June–August) is the peak of elm growth, which is considerably dependent on water availability; good water conditions during this period effectively promote the rapid growth of elm. The same is true during September. Meanwhile, the average and maximum temperatures during this period are high enough to cause severe evaporation, thereby reducing water supply and consequently, elm growth. The precipitation in July–September accounts for more of the proportion of annual precipitation, though elm growth is also dependent on rainfall occurring in other months. In other words, elm growth is most closely related to annual precipitation: the greater the annual rainfall, the faster the elm growth.

In addition, precipitation during the previous 1–2 years strongly influences elm growth. A large rainfall event in these years can substantially contribute to the groundwater supply. Good water conservation lays the foundation for succeeding years. The conservation and sustained growth of elm depends on the abundance of water resources during previous years.

The monthly minimum temperature over the previous 1–2 years also has a significant effect on elm growth. Thus, low temperatures during summer result in less evaporation and better water conservation. Although elm may exhibit more gradual growth during winter in arid and semi-arid regions, it still requires abundant water, making low temperatures during this season equally conducive to elm growth. Temperature differentially affects vegetation at varied stages, especially in the current context of climate anomalies (Zhao et al. 2008). The role that temperature plays becomes increasingly important.

Overall, elm trees in the study area are affected primarily by precipitation, average temperature, maximum temperature, minimum temperature, and the combined effects of heat and water.

## 3.2 Reconstruction of average minimum winter temperature

In accordance with the response relationship, we reconstructed the average minimum winter (The winter means from December to February, namely December in this year and

**Fig. 3** Correlation coefficients among standard chronological sequences and standard chronological year $t$+1 and year $t$+2 sequences for monthly minimum temperature, average temperature, monthly max temperature, and monthly precipitation

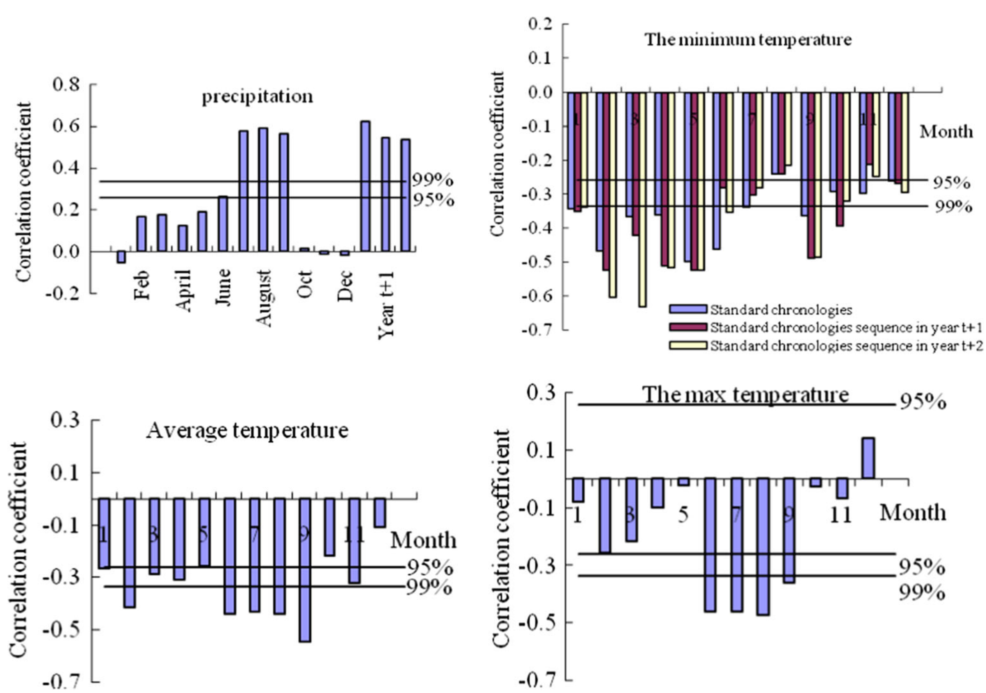

January and February in the next year. The average minimum temperature in winter is the average of monthly average daily minimum temperature in these 3 months.) temperature from 1826 to 2006 using the standard chronological sequence and standard chronological $t$+1 and $t$+2 sequences in relation to the study area. The following equation was adopted:

$$TL_t = -12.51 - 0.53 \times I_t - 1.48 \times I_{t+1} - 2.24 \times I_{t+2}$$

($N$=55, $r$=0.68, $R^2$=0.46, $R^2_{adj}$=0.40, $F(3,51)$=7.27, $P$<0.001)

where $TL_t$ is the average minimum winter temperature (°C) in year $t$; $I_t$ denotes the index of standard tree ring chronology in year $t$ (dimensionless); $I_{t+1}$ is the index of standard tree ring chronology in year $t$+1 (dimensionless); and $I_{t+2}$ is the index of standard tree ring chronology in year $t$+2 (dimensionless).

The reconstructed sequence exhibited a similar trend as the corresponding measured values, though some extreme values were not completely consistent with the reconstructed values. That is, part of the tree ring reconstruction results underestimated extreme weather events (Fritts 1976), particularly extremely cold years. However, the reconstruction equation yielded similar results for the reconstruction of the average minimum winter temperature. The reconstructed and measured values exhibited positive synchronization.

Additional tests on the stability and reliability of the reconstruction equation are necessary to ensure the credibility of the reconstruction value when a value generated beyond the calibration period is used. The one-out method was used to calculate the six parameters of the indicators and cross-test the reconstruction equation. Table 2 shows the calculated parameters.

The table shows a reduction error (RE) of 0.33, which is greater than 0.3. When the RE value is higher than 0.3, the reconstruction value is considered credible (Li et al. 2000). The correlation coefficient of cross-examination and the cross-examination of the first-order correlation coefficient were 0.591 and 0.622, respectively. These values were significant at the 0.05 level. The sign test results for the original and first-difference sequences of symbols were 40/55 and 38/54, respectively. These were significant at the 0.05 level, indicating that the reconstructed and measured value sequences were in agreement with the changes in the high frequencies and low frequencies. The average test value for the product was 3.03, which was significant at the 0.05 level, indicating a significant difference between the identical and opposing serial number sequences. All the parameters indicated that the reconstruction equation was stable and reliable and that the reconstruction results for the average minimum winter temperature derived from this equation were credible.

Thus, the average minimum winter temperature series for the Horqin Sandy Land from 1826 to 2006 was rebuilt according to the reconstruction equation. The reconstruction sequence is shown in Fig. 4.

**Table 2** Characteristic parameters for the winter average minimum temperature reconstruction equation

| $RE$ | $r$ | $r_d$ | $Z$ | $Z_d$ | $t$ |
|---|---|---|---|---|---|
| 0.33 | 0.591 | 0.622 | 40/55 | 38/54 | 3.03 |

where $RE$ is the error of reduction; $r$ is the correlation coefficient of cross-examination; $r_d$ is the cross examination of the first-order correlation coefficient; $Z$ is the value of the sign test results for the original; $Z_d$ is the first difference sequence of symbols for the test results; $t$ is the average test value for the product

## 4 Variation characteristics of average minimum winter temperature

The changes in the average minimum winter (December, the following January, and February) temperature in the study area for the past 181 years were reconstructed. These changes revealed strong low-frequency information, as shown in Fig. 4, which also indicates a linear trend among the variations.

Sequence graphs of the surface reconstruction value sequence, reconstruction from the average value, and surface reconstruction value for every 10-year average value were mapped to clearly determine the height phase changes in the temperature reconstruction sequence (Fig. 5). In addition, a low-pass filter, whose length was 13, was used to filter less than 8 years of high-frequency wave. The temperature curve is also shown in Fig. 5.

Furthermore, Fig. 5 illustrates that the average minimum winter temperature in Sandy Land generally experienced moderate fluctuations. The warmest year in the entire reconstruction period was 2004, whose average minimum temperature was −15.36 °C. The coldest year was 1830, whose average minimum temperature was −19.71 °C, followed by 1957 with an average minimum temperature of −19.7 °C. The temperature differences between the two coldest years were non-significant. The warmest 10 years occurred during the 2000s, and the coldest occurred in the 1950s. The temperature fluctuations from 1826 to 1923 were moderate, showing small changes in the overall trend. Years 1826–1830, 1837–1859, 1864–1875, and 1883–1905 were in the cooling stage, whereas 1830–1837, 1859–1864, 1875–1883, and 1905–1923 were in the warming stage. Extensive cooling was observed from 1923 to 1957 and considerable warming was observed in 1957–2006.

The longest continual cooling time period occurred from 1923 to 1957 (35 years) followed by 1837 to 1859 (23 years). The two longest continual heating time periods lasted for 50 (1957–2006) and 19 years (1905–1923). During the reconstruction of the entire minimum temperature period, the

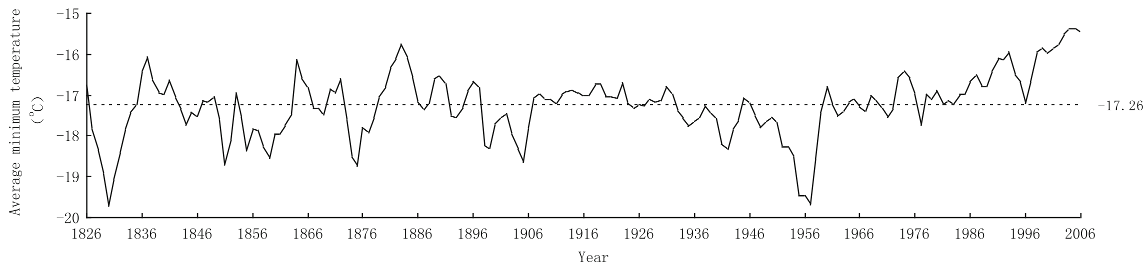


**Fig. 4** Reconstruction of winter (Dec, Jan, and Feb) average minimum temperature

average minimum temperatures in the gentle wave, intense cooling, and considerable heating stages were −17.35, −17.69, and −16.81 °C, respectively. The average temperature was −17.26 °C. That is, after 1957, the average minimum winter temperature began to greatly increase. The average temperature in 1957–2006 was higher than that recorded for the past 181 years, in which a mean maximum of −15.61 °C was observed in 2000.

The different frequencies of changes in the mean minimum temperature of the years studied were analyzed using a 0.5 interval in the temperature ranges (Fig. 6). The different stages were not significantly different than normal distributions. Additionally, positive and negative interval statistics were examined. From 1826 to 1923 (98 years), 47 years (48 %) corresponded to the negative interval with a lower-than-average temperature and 51 years (58 %) corresponded to the positive interval, indicating a balance between the positive and negative years.

From 1924 to 1957 (34 years), 24 years (70.59 %) accounted for the negative interval while 10 years (29.41 %) accounted for the positive interval, which is far less than the proportion of negative years. From 1958 to 2006 (49 years), 10 years (20.41 %) and 39 years (79.59 %) accounted for the negative and positive intervals, respectively. The latter accounted for a much higher proportion than did the negative years. From 1826 to 2006 (181 years), 81 years (44.75 %) corresponded to the negative interval and 100 years (55.25 %) corresponded to the positive interval. The number of years in the positive interval is slightly higher than that under the negative interval.

The entire reconstruction period of the 10-year average minimum temperature differences among the inter-annual changes was analyzed (Fig. 7). The magnitude of change was more moderate, and the relative amplitude was slightly larger during the 1960s. The changes in amplitude yielded a positive value after the 1950s, demonstrating an increasing trend. The amplitude lay between 0.136 and 1.285 °C during the entire period, changing little from the 1960s to the 1970s with a temperature increase of 0.136 °C. The largest change in value occurred in the 1950s–1960s, with a maximum temperature rise of 1.285 °C. This increase is a turning point (1957), given the sharp rise. The second rapid warming stage occurred in the 1870s–1880s, with a temperature of up to 0.966 °C. The third stage of rapid warming occurred in the 1990s–2000s, with a temperature increase of 0.734 °C. Therefore, during the 1950s–2000s (50 years), the warming trend rate was 0.575 °C/10 years, while the overall temperature rise was 1.543° over the entire 50 year period.

The aforementioned results for the minimum temperature variations are similar to those found in the previous studies in Northern China (Zhai and Pan 2003; Wang et al. 2004a), regions of China (Xun et al. 2004), the northeastern climate and ecological transition zone (Zhang and Zhang 2005), and Horqin Sandy Land (Yi et al. 2006). For 1959–2002 (44 years), Sun et al. (2006) reported that the northeastern region exhibited a significant warming trend for the

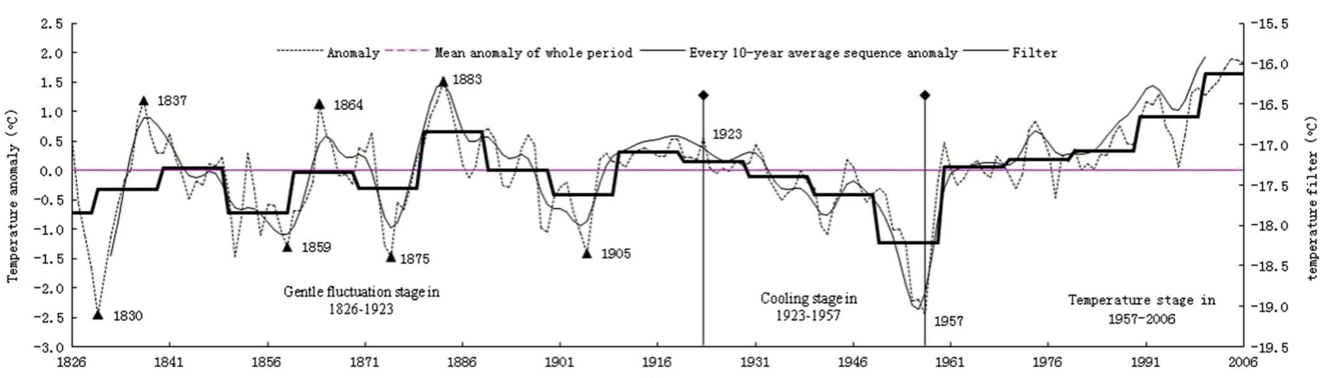


**Fig. 5** The anomaly sequence, average range, every 10-year average sequence anomaly, and filter curves of the winter (Dec to Feb) average minimum temperature

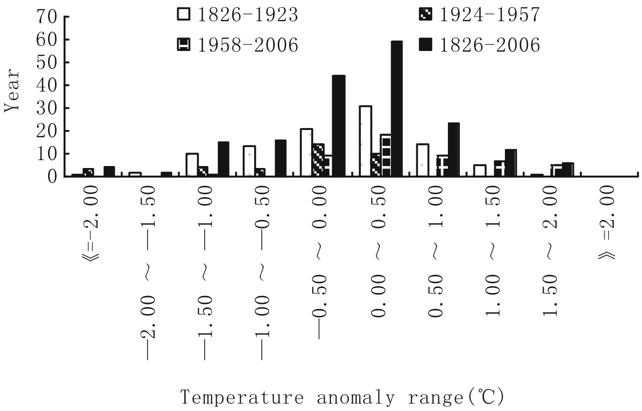


**Fig. 6** Reconstructed average winter minimum temperature anomaly sequence of the different number of frequency changes in the temperature range

maximum and minimum temperatures and that a clear peak of warming has recently been observed. In addition, the increasing trend of the minimum winter temperature is more pronounced than that of the maximum temperature during summer; the strong warming area is located mainly in Horqin Sandy Land, which is on the border of Inner Mongolia. Hou et al. (2006) stated that the annual average temperature in Northeastern China increased from 1951 to 2003. Moreover, Wang et al. (2007a) showed that since 1957, an increasing trend in the daily maximum and minimum temperatures has occurred over time in the Wengniute Banner in Sandy Land and that the daily minimum temperature increments is 11 times higher than the maximum temperature increments. After the 1980s, the maximum and minimum temperatures significantly increased. The study also suggests that the temperature series in 25 years (1981–2005) is indicative of a non-continuous upward trend in the Aogula Ulam area of Sandy Land (Wang et al. 2007b) and that the warming was significantly asymmetric. Liang et al. (2009) concluded that the temperature increased 0.28 °C/10 years from 1951 to 2006 in Horqin Sandy Land; this value is much higher than the

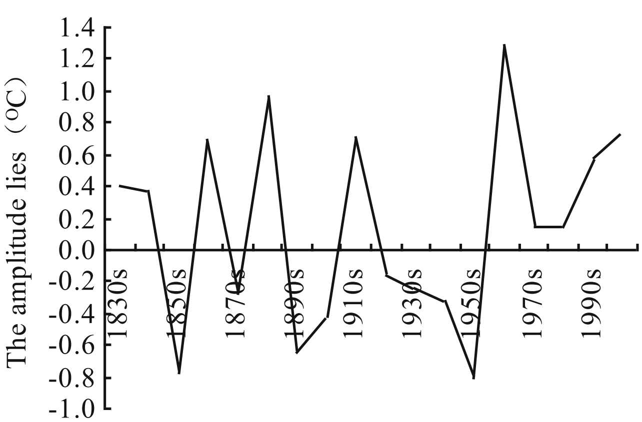


**Fig. 7** Inter-annual variation in mean winter minimum temperature averaged over 10-year time spans for the entire reconstruction period

average warming rate of 0.13 °C/10 years observed over nearly 50 years around the world. Each season, temperature exhibited an upward trend. The winter warming rate was 0.46 °C/10 years, which is extremely significant. The annual maximum (0.17 °C/10a) and minimum (0.42 °C/10a) temperatures both exhibited a remarkable rise.

## 5 Discussion and conclusion

The average minimum winter temperature of Horqin Sandy Land was reconstructed using the tree ring width chronology of elm. The reconstructed and measured values are consistent with the calculated results. Various test findings show that the reconstruction results were stable and reliable.

The average minimum winter temperature of the study area experienced a moderate fluctuation stage (1826–1923), substantial cooling stage (1923–1957), and considerable warming stage (1957–2006) across nearly 180 years. Clearly observable changes in the process were found.

In the reconstruction sequence of the average minimum winter temperature, the warmest year was 2004 (−15.36 °C) and the coldest was 1830 (−19.71 °C; −19.70 °C in 1957). Moreover, the 10 warmest years occurred in the 2000s and the coldest occurred in the 1950s.

During the phases of change in the gentle fluctuation, substantial cooling, and considerable warming stages, the minimum temperatures were −17.35, −17.69, and −16.81 °C, respectively, with an average of −17.26 °C. The average value in the past 50 years is higher than any of those observed during the reconstruction period.

The abovementioned results show that the change in the 10-year average rate of the minimum temperature was more moderate, including the most remarkable variation in the 1950s–1960s, with a maximum warming rate of 1.285 °C. This rate is a turning point (1957) given the sharp temperature rise. The second rapid warming stage occurred during the 1870s–1880s, and the third occurred during the 1990s–2000s. Overall, the rapid heating process during the 1950s–2000s exhibited a higher heating rate than those observed in the reconstruction period. The warming trend rate was 0.575 °C/10 years, and the total temperature rise was 1.543 °C. The continued increase in the minimum temperature in these areas is expected to cause ecological and environment problems of a wider and longer-scale scope. These problems will further affect living environments and human activities.

**Acknowledgments** This research was supported by the Inner Mongolia Autonomous Region Innovation team on water resources efficiency of semi-arid regions affected by hydrological processes and its regulation technology, Inner Mongolia Natural Science Fund Projects (Grant No: 2014MS0407, 2010BS0608), and the National Natural Science Funds Projects (Grant No: 50869005).

## References


Cook ER, Jacoby GC (1983) Potomac river stream flow since 1730 as reconstruction tree rings. J Clim Appl Meteorol 22:1659–1672

Chen LX, Zhou XJ, Li WL, Luo YF, Zhu WQ (2004) Characteristics of the climate change and its formation mechanism in China in last 80 years. Acta Meteorol Sin 62(5):634–646

Ding YH, Ren GY, Shi GY, Gong P, Zheng XH, Qu PM, Zhang DE, Zhao ZC, Wang SW, Wang HJ, Luo Y, Chen DL, Gao XJ, Dai XS (2006) National assessment report of climate change (I): climate change in China and its future trend. Adv Clim Chang Res 2(1):3–8

Dong GR, Jin HL, Chen HZ, Zhang CL (1998) China northern half dry and subhumid regions of the cause of desertification. Quat Sci 2: 136–144

Esper J, Cook ED, Schweingruber FH et al (2003) Test of the RCS met hod for preserving low-frequency variability in long tree-ring chronologies. Tree-Ring Res 9(2):81–98

Fritts HC (1976) Tree ring and climate. Academic, London, pp 1–500

Giovanna B, David F et al (2010) Five centuries of Central European temperature extremes reconstructed from tree-ring density and documentary evidence. Glob Planet Chang 72:182–191

Hou YL, Li DL, Shi YF, Shen YP (2006) Variation of annual mean temperature in northeast of China and its responding to the northern hemisphere warming and snow cover area changing in Eurasia. J Glaciol Geocryol 28(6):900–908

Jiang DM, Liu ZM, Cao YC et al (2003) Study on desertification and its restoration of Keerqin sandy land. China environmental science press, Beijing, pp 32–39

Karl T, Jones P, Knight R et al (1993) A new perspective on recent global warming: asymmetric trends of daily maximum and mini-mum temperature. Bull Am Meteorol Soc 74(6):1007–1023

Law BE, Turner D, Lefsky M et al (2006) Carbon fluxes across regions: observational constraints at multiple scales. In: Wu J, Jones B, Li H et al (eds) Scaling and uncertainty analysis in ecology: methods and applications. Columbia University Press, New York, pp 167–190

Li AM, Han ZW, Huang CH, Tan ZH (2007) Remote sensing monitoring on dynamic of sandy desertification degree in Horqin Sandy Land at the beginning of 21st century. J Desert Res 27(4):546–551

Li JF, Yuan YJ, You XR et al (2000) Tree-ring research and application of hydrology. China environmental science press, Beijing, pp 106–107

Liang CP, Xin GD, Wang AZ, Jin CJ, Yuan FH, Wu JB, Ni P (2009) Characteristics of climate change in Horqin Sandy Land in past 56 years. Chin J ecol 28(1):2326–2332

Ma L, Liu TX, Ji HL, Luo YY, Duan LM, Yang Y (2011) Establishment of ring width chronology and reconstruction of Ulmus pumila L.in Horqin Sandy Land since 1826. Quat Sci 31(2):360–369

Ma L, Liu TX, Kou ZQ, Kang CF (2007) Relationship of elm growth and hydrometeorological factors of Horqin Sandy Land and climatic series reconstruction. J Glaciol Geocryol 29(5):802–807

Ma XB (1999) Asymmetric trend of maximum and mini-mum temperature change in northwest China. J Meteorol 57(5):613–621

Magda VN, Zelenova AV, Andreev SG (2001) A 280-year reconstruction of Baikal Lake water level from treerings. Confercnce "Tree Rings and Peopl" 22–26

Nicoletta M (2004) Climate from dendrochronology: latest developments and results. Glob Planet Chang 40:129–139

Shao XM (1997) Some development of chronology round the tree. Quat Sci 3:265–271

Shao XM, Wang SZ, Xu Y, Zhu HF, Xu XG, Xiao YM (2007) A 3500-year master tree-ring dating chronology from the northeastern part of the Qaidam Basin. Quat Sci 27(4):477–485

Stockton CW, Meko DM (1975) A long-term history of drought occurrence in western United States as inferred from tree rings. Weatherwise 28(6):245–249

Sun FH, Yang XQ, Lu S, Yang SY (2006) The contrast analysis on the average and extremum temperature trend in northeast china. Sci Meteorol Sin 26(2):157–163

Van Arsdale RB, Stahle DW, Cleaveland MK (1998) Earthquake signals in tree-ring data from the New Madrid seismic zone and implications for paleoseimicity. Geology 26(6):515–518

Wang SW (1994) Introduction to the climate system. China meteorological press, Beijing, pp 54–59

Wang T, Zhu ZD (2001) The desertification problems of northern China. Quat Sci 21(1):56–65

Wang HM, Luo YM, Jiang DM (2007a) Unsymmetrical variation of the maximum and minimum air temperatures in Wengniute Banner, Horqin Sandland. Arid Zone Res 24(2):261–267

Wang HM, Luo YM, Jiang DM (2007b) Variation trends of maximal and minimal air temperature at Wulanaodu region, Horqin steppe. Chin J Agrometeorology 28(2):124–127

Wang L, Xie XQ, Su W, Guo XB (2004a) Changes of maximum and minimum temperature and their impacts in northern China over the second half of the 20th century. J Nat Resour 19(3):337–343

Wang SW, Luo Y, Zhao ZC, Dong WJ, Yang B (2005) The dispute about climate change. Prog Nat Sci 15(8):917–922

Wang T, Chen GT, Zhao HL, Dong ZB, Zhang XY, Zheng XJ, Wang NA (2006) Research progress on aeolian desertification process and controlling in north of China. J Desert Res 26(4):507–516

Wang T, Wu W, Xue X, Sun QW, Zhang WM, Han ZW (2004b) Spatial-temporal changes of sandy desertified land during last 5 decades in northern China. Acta Geogr Sin 59(2):203–212

Wang T, Wu W, Zhao HL, Hu MC, Zhao AG (2004c) Analyses on driving factors to sandy desertification process in Horqin Region, China. J Desert Res 24(5):519–528

Wang T, Zhu ZD, Wu W (2002) Sandy desertification in the north China. Sci China Ser D 45(Supp):23–34

Wilson R, Luckman B (2003) Dendroclimatic reconstruction of maximum summer temperatures from upper treeline sites in interior British Columbia. Canada. The Holocene 13(6):851–861

Wu XD, Sun L, Zhan XZ (1989) Attempt on past climate change of central Tibet under the method of tree ring material reconstruction. Acta Geograph Sin 44(3):334–341

Xie Z, Cao HX (1996) Asymmetric trend of maximum and minimum temperature change in Beijing. J Meteorol 54(4):501–507

Xun LC, Zhou XJ, Li WL (2004) Characteristics of the climate change and its formation mechanism in china in last 80 years. Acta Geogr Sin 62(5):634–646

Yi SW, Lu HY, Zhou LY, Miao XD (2006) The wet-dry variations of the Horqin sandy field recorded by loess deposit of the late quaternare. J Desert Res 26(6):869–874

Zhai PM, Pan XH (2003) Changes on temperature and precipitation extreme events in northern china over nearly 50 years. J Geogr Sci 58(Supp):408–414

Zhang YC, Zhang LJ (2005) Precipitation and temperature probability characteristics in climatic and ecological transition zone of northeast China in recent 50 years. Sci Geogr Sin 25(5):561–566

Zhao HL, Da HJZ, Zhou RL, Li YL, Zuo XA, Huang G (2008) Effects of human activity and climate changes on vegetation in Horqin sandy grassland, inner Mongolia. Adv Earth Sci 23(4):408–414

Zhuo ZD, Hu SX, Zhang XG, Zhao Q, Wang YX, Liu GY (1979) Tree ring in the Qilian mountains and climate change of nearly one thousand years in china (1059–1975). J Lanzhou Univ 2:145–157